ROTARY REPLICATION FOR FREEZE-ETCHING

LUKAS H. MARGARITIS, ARNLJOT ELGSAETER, and DANIEL BRANTON

From the Biological Laboratories, Harvard University, Cambridge, Massachusetts 02138. Dr. Margaritis' present address is the Department of Biology, University of Athens, Panepistimiopolis, Kouponia, Athens-621, Greece. Dr. Elgsaeter's present address is the Institute of Biophysics, University of Trondheim, N-7034 Trondheim-NTH, Norway

ABSTRACT

Rotary replication has been adapted to freeze-etching and evaluated using T4 polyheads, erythrocyte ghosts, and chloroplast membranes. Conventional electron microscopy, electron diffraction, and optical diffraction and filtering indicate that platinum-carbon rotary replication renders radially symmetrical contrast and 25 Å resolution to freeze-etched specimens so as to clarify subunit structure not normally evident in unidirectional shadow replicas.

Freeze-etching has exposed many new details of cell and membrane organization, but the unidirectional shadow method of replication most commonly used with the technique does not contrast surface relief in all directions. Furthermore, a unidirectional shadow cast by one structure may obscure a neighboring structure and make it difficult to discriminate contiguous elements. These limitations on contrast and visibility may be as important as the inherent limitation of resolution in restricting the information which can be derived from an electron micrograph of a freeze-etched specimen.

The limitations of unidirectional shadowing have long been recognized (14) and may be overcome by using rotary replication. However, the mechanical and temperature control required during freeze-etching make it difficult to rotate a hydrated, frozen, fractured specimen. By employing magnetic rather than mechanical coupling to affix the specimen carrier to the cold specimen table, we have been able to construct a stage that satisfies the usual requirements for freeze-etching and also allows specimen rotation during the shadowing. We evaluated this rotary replication technique by conventional electron microscopy and electron and diffraction analyses of the replicas. We also tested a variety of heavy metal shadowing materials and configurations. Our results show that platinum-carbon rotary replication renders radially symmetrical contrast and 25 Å resolution to freeze-etched specimens so as to clarify structural features difficult or impossible to discern in unidirectionally shadowed specimens.

MATERIALS AND METHODS

Biological Materials

Ghosts of human erythrocytes were prepared by hypotonic lysis (8). Chloroplasts were isolated from barley (*Hordeum vulgare* L.) in 300 mM NaCl, 50 mM Tricine (California Biochemical Corp., Los Angeles, Calif.), 2 mM $MgCl_2$, pH 7.5, and swollen, washed, and harvested in 5 mM Tricine, 2 mM $MgCl_2$. Droplets of the washed ghosts in 20 mosmol sodium phosphate buffer, pH 7.6, or of the chloroplasts in final Tricine-$MgCl_2$ wash were frozen for freeze-etching without further treatment (9).

Polyheads of T4 mutant 20 (αmN50) were isolated from infected *Escherichia coli* strain B cells as described by Laemmli and Ouittner (11). The final pellet containing the polyheads was washed three times with distilled water and small samples were frozen for freeze-etching.

Rotary Shadow Unit

The standard Balzers specimen stage (Balzers High Vacuum Corp., Santa Ana, Calif.) was replaced by a

cobalt-samarium pot magnet that served to hold down a tooth-wheeled specimen carrier, the specimen on its specimen support, and a holding plate (Figs. 1 and 2). During heavy metal evaporation, a toothed gear-wheel, coupled via a feed-through to an electric motor outside the vacuum system, caused the specimen carrier, specimen, and holding plate to rotate on the liquid N_2 cooled pot magnet. A fine powder of molybdenum disulfide between the magnet and the specimen carrier served to lubricate the moving surfaces.

Freeze-etching

Specimens were mounted on hat-shaped colper planchets, frozen in liquid Freon-22 (E. I. duPont de Nemours & Co., Wilmington, Del.), and freeze-etching was performed in a Balzers unit as described (9), except that in many experiments, the specimens were rotated during shadow-casting from electron bombardment units (2, 12). Before evaporation, specimens were fractured and etched at −100°C. This temperature was previously verified on the rotary specimen carrier while stationary, using a calibrated thermocouple, but it probably rose during the 10–20 s of rotation and shadow-casting.

Shadow-casting

Conventional unidirectional shadows were cast from standard Balzers electron bombardment guns set at a 25° angle to the specimen table surface. The anode materials and configurations are described in each experiment.

The anode materials were as follows (Table I): The Pt pellet, C anode consisted of a 2 × 1.5-mm diameter Pt pellet inserted in the drilled-out end of a 2 × 20-mm C-rod. The Pt-C compound was a mixture of approximately 50% C-50% Pt in a rod form (Polysciences, Inc., Paul Valley Industrial Park, Warrington, Pa. catalog no. 2947). The other anodes were either pure platinum or platinum-iridium (80:20) and platinum-palladium (80:20) alloys of 0.2 mm (0.008 inch) diameter wound around the 0.5 mm (0.020 inch) tip of a 2 mm-thick tungsten rod, or inserted as a coil inside the drilled-out end of a 2 × 20-mm carbon rod.

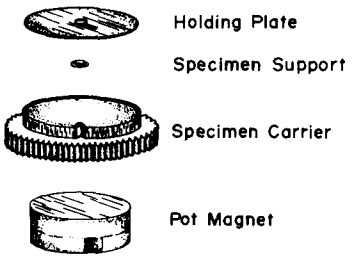

FIGURE 1 Rotary replication unit. Either single specimen holding plates with one hole (shown here) or multiple specimen holding plates with four holes (Fig. 2) were used. The pot magnet was a cylindrical cobalt samarium Gecor magnet, (General Electric Co., Magnetic Materials Section, Edmore, Mich.) surrounded by a vanadium Permendur (Allegheny Ludlum Steel Corp., Pittsburgh, Pa.) pot.

For rotary replication the electron bombardment gun (platinum pellet-carbon rod anode) was set at an angle of 6° (chloroplasts), 12° (polyheads), or 16° (erythrocyte ghosts) to the specimen table surface. The replica was reinforced with carbon from a second electron bombardment gun positioned above the specimen.

Trial and error with each new shadow-casting method or anode configuration indicated the optimum replica thickness, which was measured with a film thickness monitor (Balzers High Vacuum Corp.). Only the replicas of optimal thickness were used for the comparative evaluations of replica quality.

Electron Microscopy

The replicas, on bare 400-mesh grids, were examined in a Philips 301 electron microscope with an anticontamination device at an accelerating voltage of 80 kV. Magnification was calibrated with a carbon diffraction grating replica (28,800 lines/inch, Ladd Research Industries, Inc., Burlington, Vt.).

Selected area electron diffraction was used to monitor the degree of crystallization in the replicas, after one or more exposures of the replica area to a standardized dose of electrons. Lacking a Farady cage, we approximated a standardized electron dosage with the microscope photometer. This was done by adjusting the emission current and second condenser so that in the standard operating mode, with the lenses set at a magnification of 25,000:1 and the emulsion sensitivity control set at 2, the microscope photometer indicated that a 2-s exposure would be required for a photograph. As soon as a fresh area of the replica was positioned under the beam, the microscope, with no other settings changed, was switched to the diffraction mode, and exposure of a photographic plate to the diffraction pattern commenced and continued for 8 s. The micrograph so produced was taken to represent the degree of crystallization in the replica after one standard dose of electrons. The degree of crystallization detected by the diffraction pattern was scaled by visual comparison with four arbitrarily chosen diffraction patterns of an initially low crystallinity replica which had been subject to 1, 20, 100, and 200 standard doses of electrons (Fig. 3). When we took an electron micrograph of the image of a replica, as opposed to the diffraction pattern of a replica, the photographed area of the replica was subjected to approximately one standard dose of electrons which allowed sufficient time to focus and expose the plate.

All electron micrographs except the filtered images are positive images, i.e., platinum deposits appear dark. The direction of heavy metal evaporation is shown by an arrow at the lower right of each figure. The angle between the electron bombardment gun and the specimen table surface is shown inside the rotary arrow which designates rotary replication.

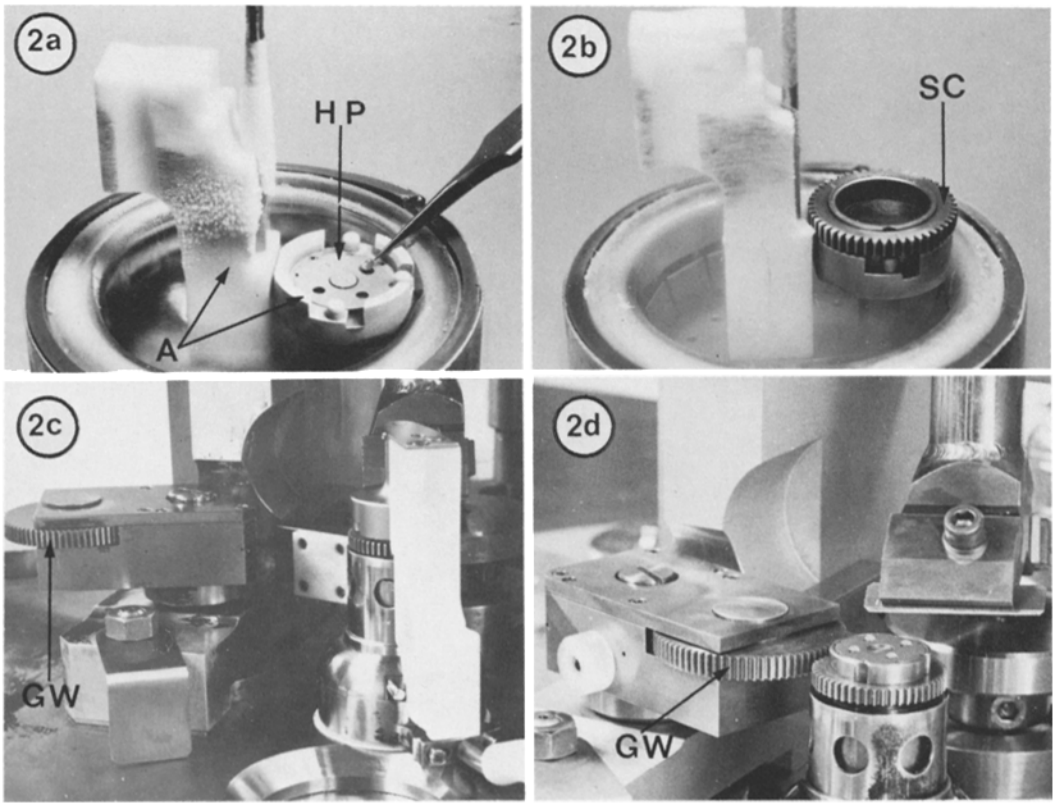

FIGURE 2 Use of the rotary replication unit. (*a*) Specimens, mounted and frozen on hat-shaped specimen supports (9), were placed, specimen side down, into the holes of the cold holding plate. The holding plate (*HP*) was held in a liquid N_2-filled Dewar flask by an applicator (*A*). An ordinary, small, cylindrical magnet in the applicator centered the holding plate in position. (*b*) After loading the holding plate with specimens, the precooled specimen carrier (*SC*) was placed, upside down, into the applicator. The rim of the specimen supports was now sandwiched between the holding plate and the specimen carrier. The specimen carrier was held in position by the cylindrical magnet in the applicator. (*c*) The entire applicator, with specimen carrier, specimens and holding plate, was removed from the Dewar flask, inverted, and lowered onto a pot magnet which replaced the normal specimen stage in the freeze-etch machine. (*d*) When the applicator was removed, the holding plate, specimens, and specimen carrier were held down by the strong magnetic field of the pot magnet which overcame the weaker magnetic attraction of the cylindrical magnet in the applicator. Rotation of the specimen carrier, specimens, and holding plate was affected by the toothed gear wheel (*GW*) which was swung out of position (Fig. 2*c*) at all times and engaged (Fig. 2*d*) only during shadowing. The toothed gear wheel and its housing were designed so that its rotation and its movement to engage or disengage the specimen carrier were driven by rotation of the same feed-through which served as the central shaft on which the toothed gear wheel housing was mounted. Stainless steel construction minimized heat transfer between the toothed gear wheels and prevented substantial heat transfer during the short time (less than 30 s) required to cast the rotary replica.[1a]

Image Analysis

Optical diffraction patterns from representative polyheads were obtained using a helium-neon laser (7). The patterns could be indexed on the expected reciprocal hexagonal lattice (7) and in many cases showed third and fourth order spots corresponding to 35 and 25 Å, respectively. The highest angle lattice spots reproducibly found in diffraction patterns from a replica were taken to indicate the resolution in that particular replica.

In some cases, the polyhead was reconstructed from its filtered diffraction pattern (7). The filtering masks were prepared by photoetching.[1]

[1a] Balzers, AG will shortly market a commercial version of our rotary replication device.

[1] David J. DeRosier. Personal communication.

TABLE I

Relationship between Grain Size, Platinum Crystallization, and Replica Resolution with Different Replicating Material

Anode	Grain size (± 20%)	Crystallization*		Resolution
		Initial	Final	
	Å			Å
Pt pellet, C 	25	Moderate	High	25
Pt-C compound 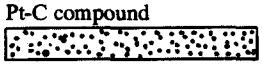	15	Very low	"	50
Pt+Ir wire, C 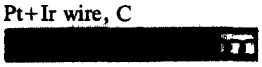	20	Low	"	25
Pt wire, W 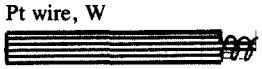	25	Moderate	"	25
Pt+Ir wire, W 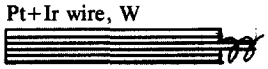	20	Moderate	"	25
Pt+Pd wire, W 	>25	Moderate	"	50

* Initial crystallization represents the degree of crystallization after 1 standard dose of electrons; final crystallization, after 200 standard doses. Designations of very low, low, moderate, and high refer to the scale established by the reference patterns shown in Fig. 3.

RESULTS

Rotary replication disclosed the structure of the erythrocyte intramembrane particles (Figs. 4*a* and *b*) and chloroplast lamellae surface particles (Figs. 5*b* and *c*) with a clarity usually unattainable by unidirectional shadowing (Fig. 4*b* inset, Fig. 5*a*). The presence of subunits, often in a clear tetrameric arrangement (circles, Fig. 4*b*), was particularly striking in the erythrocyte membrane, where we had not been able to discern such detail by unidirectional shadowing. However, the heterogeneity in both size and subunit arrangement within the population of erythrocyte intramembrane particles was surprising and led us to question the validity of interpretations based on rotary replication. In particular, we asked ourselves whether improvement of unidirectional shadowing might achieve results equivalent to those of rotary replication or whether some process inherent in the crystallization of the platinum-carbon replica might be producing a misleading artifact.

Although improvements in the resolution attainable from heavy metal replicas have been discussed (12, 14), we could not find a systematic evaluation of the various heavy metal mixtures and source configurations which have been proposed. We therefore undertook such an evaluation and selected T4 polyheads as a model system because their surface structure has been well characterized (7), is amenable to optical analysis, and contains capsomeric units whose size (≃60 Å) is close to or even smaller than that of many intramembrane particles. Our evaluation was based on electron diffraction of the T4 polyhead replicas to assay platinum crystallinity, direct measurement on the electron micrographs to determine grain size, and optical diffraction of the micrographs to establish resolution limits.

An electron micrograph of a representative platinum pellet, carbon anode replica and its optical transform (Fig. 6) is illustrative of our results, which are summarized in Table I. Our results show that segeral platinum-heavy metal or platinum-carbon combinations produce replicas that resolve 25 Å periodicities. Perhaps because of somewhat smaller background granularity, the iridium-containing anodes produced replicas which sometimes appeared clearer than those produced by the other combinations. However, this apparent improvement in the quality of iridium containing replicas was inconsistent. Furthermore,

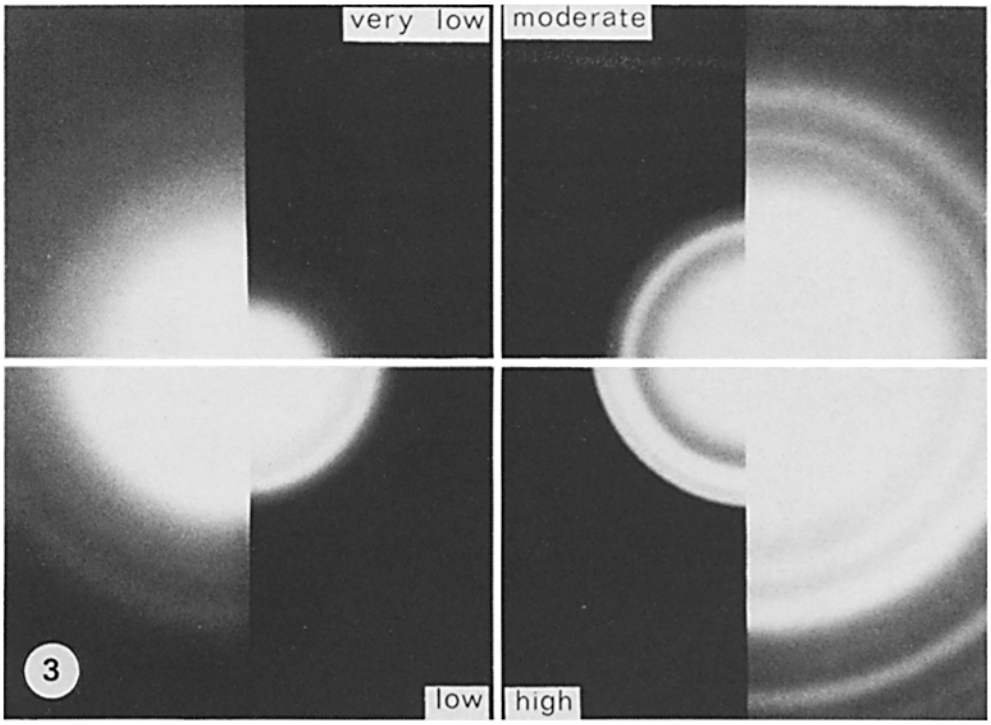

FIGURE 3 Selected area electron diffraction pattern demonstrating the polycrystalline nature of the replica. Four successive patterns are shown of a very low crystallinity replica after 1 (very low), 20 (low), 100 (moderate), and 200 (high) standard doses of electrons. Half of the print in each pattern has been doubly exposed so that the strong low order reflections will become visible. Absence of rings indicates amorphous replica structure whereas fully developed rings are indicative of the face-centered cubic lattice of platinum (13). Intermediate patterns correspond to partially crystallographically oriented platinum atoms.

comparison of results obtained from the platinum-carbon compound anode with those obtained from the platinum and palladium, tungsten anode showed that resolution cannot be related to grain size in any simple manner.

In all cases, crystallization of the replicas was promoted by exposure to the electron beam of the microscope. But, the resolution in replicas of very low initial crystallinity was no better, and in one case (platinum-carbon compound anode) was far worse than in initially moderately crystalline replicas. Furthermore, optical diffraction and direct measurement of the same polyhead, after one and again after 200 standard doses of electrons, failed to detect any change in resolution or in visible grain size concomitant with evident increases in crystallinity detected by electron diffraction. Thus, the crystallinity of the replica was independent of replica resolution and even of replica granularity, and increases in crystallinity did not lead to any image deterioration detectable by eye or by optical diffraction. Of the heavy metal combinations capable of resolving 25 Å periodic detail in the polyheads, the Pt pellet, carbon anode advocated by Moor (12), provided the most favorable combination of resolution, reasonable granularity and reproducibility. Although we attempted to evaluate the tantalum-tungsten anode advocated by Bachmann et al. (3), overheating and other problems prevented us from obtaining useful replicas with the Balzers guns at our disposal.

Having ascertained that the quality of replicas produced by unidirectional shadowing could not be improved by using other easily accessible heavy metal mixtures or anode configurations, and having assured that electron beam-induced crystallization could not account for the substructure or the heterogeneity of the rotary replicated membrane

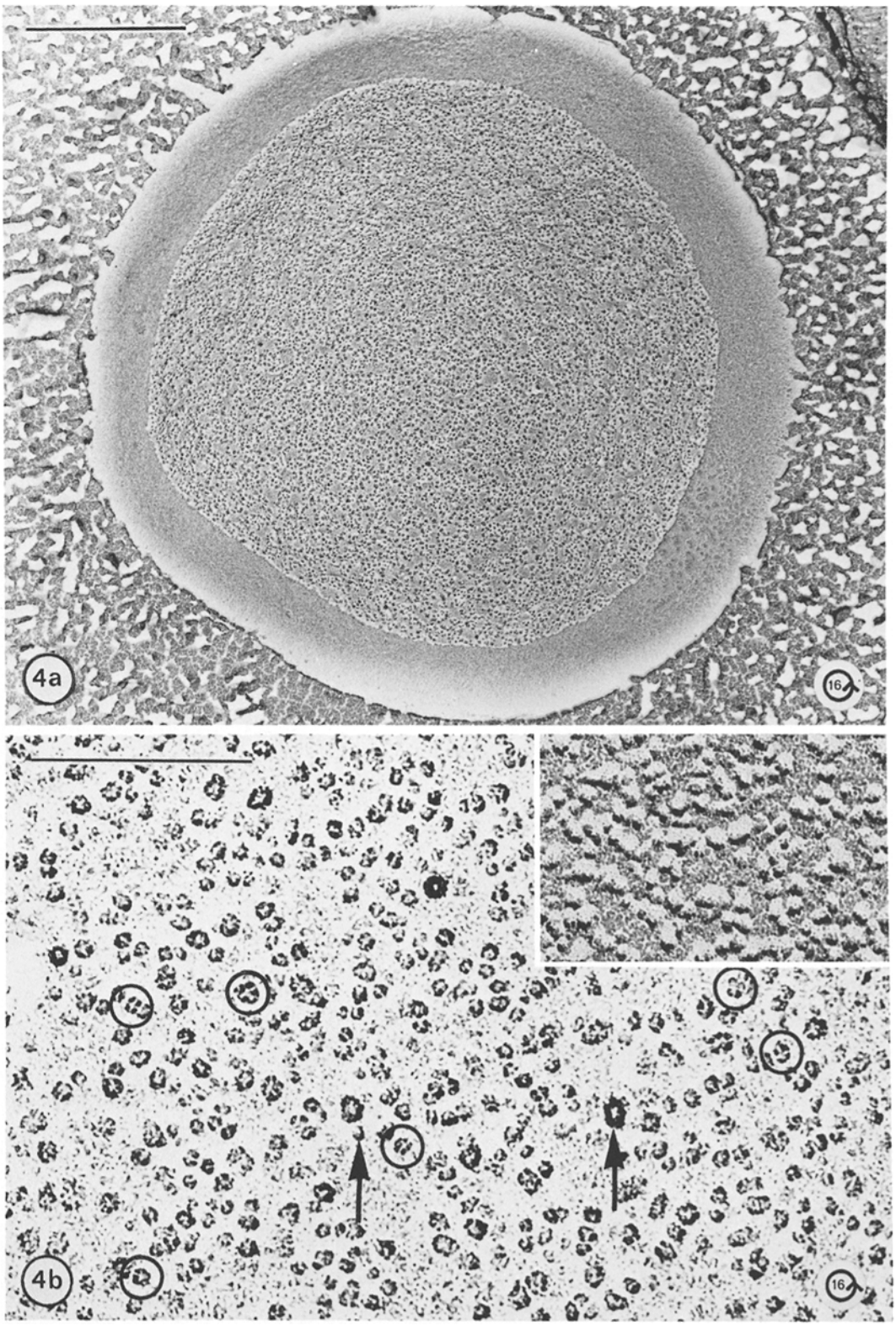

FIGURE 4 Freeze-etched erythrocyte ghost after rotary replication. (*a*) The overall contrast is high compared to that of conventional unidirectionally shadowed membranes. Bar, 0.5 μm (× 50,000). (*b*) At high magnification many of the intramembrane particles exhibit tetrameric subunit structure (circles) normally not visible after conventional unidirectional shadowing. However, heterogeneity in size and substructure is also evident (arrows). Bar, 0.1 μm (× 310,000).

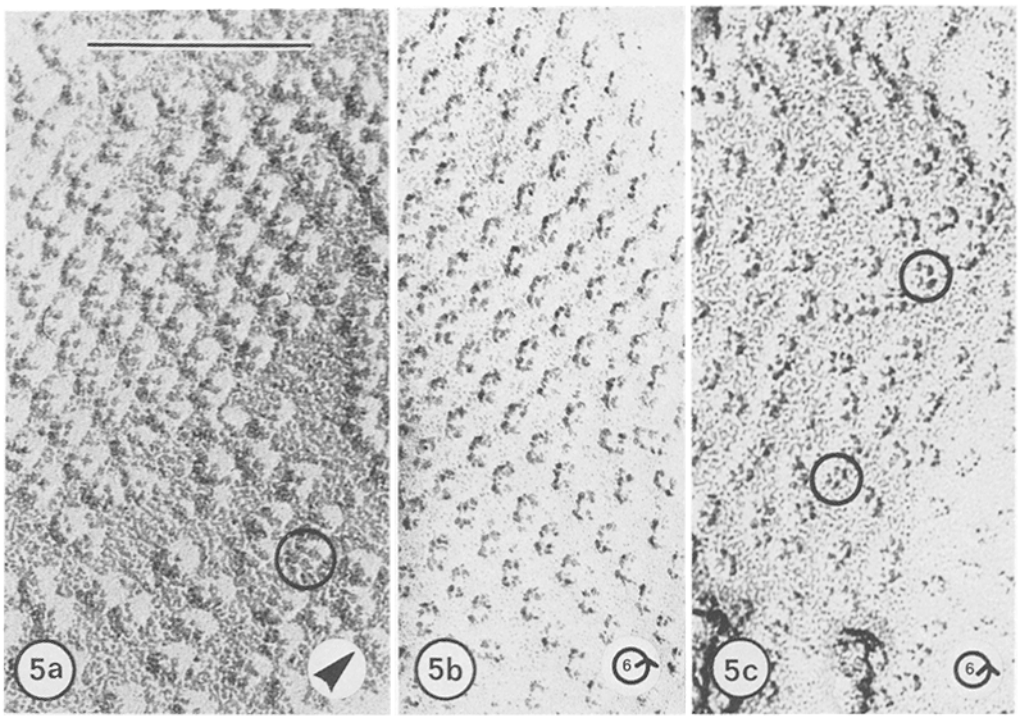

FIGURE 5 Freeze-etched E surface of chloroplast thylakoid membranes after (*a*) unidirectional and (*b* and *c*) rotary replication. Subunit structure is occasionally resolved with unidirectional shadowing (Fig. 5*a*, circle), but with rotary replication the four subunit structures of many individual particles are clearly demonstrated (Fig. 5*c*, circles). Note that the interparticle spacing (240 × 180 Å) in *a* and *b* are identical although the particles appear to be much larger in *a*. Bar, 0.1 μm (× 280,000).

particles, we chose to use the standard Pt pellet, carbon anode in rotary replica experiments with our model system of T4 polyheads.

Optical transforms of representative micrographs (Fig. 7) showed that the resolution of rotary replicas was equivalent to that of unidirectionally shadowed specimens. However, in contrast to the unidirectional shadow-replicas, rotary replicated polyheads show hexagonally arranged capsomeric subunits which can be directly visualized in the original micrographs (compare Fig. 6*a* with Fig. 7*a*) and the optical transforms contain reciprocal lattice spots whose intensity is more uniform around the undiffracted beam (compare Fig. 6*b* with Fig. 7*b*).

We subsequently used optical filtering to facilitate direct comparison between our rotary shadowed replicas and previously published filtered images of the near surface of negatively stained polyheads. With negatively stained material, optical filtering is necessary to distinguish the superposed near- and far-side images. But optical filtering also eliminates random noise from the image. Thus, although there is no problem with superposition of near- and far-side images in freeze-etching, a fair comparison between a replica and a near-side (hence optically filtered) negative stain image requires that the replica image also be filtered. In general, the filtered images of unidirectionally shadowed material revealed capsomeres which showed less detail than those produced by rotary replicated structures. However, on rare occasions, the filtered image of a unidirectionally shadowed polyhead (Fig. 8*a*) was comparable to the routine rotary-shadowed one (Fig. 8*b*), and both were very similar to the filtered image of negatively stained material (Fig. 8*c*).

DISCUSSION

Our results show that rotary shadowing can be used with freeze-etching to elucidate structural details and relationships which are not usually evident after unidirectional shadowing. Although we do not yet understand all of the physical proc-

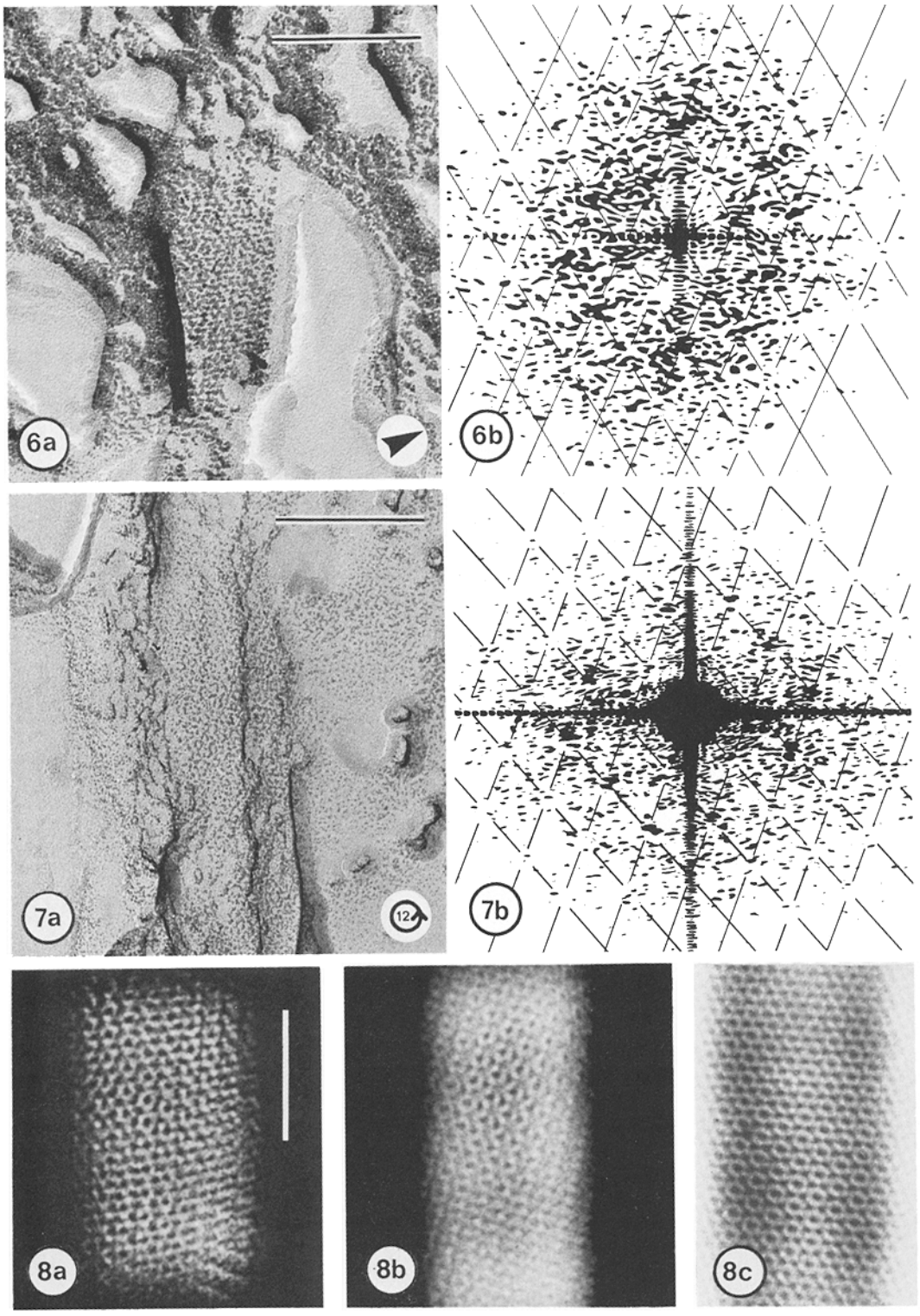
6a
6b
7a
12
7b
8a
8b
8c

esses which lead to such striking images as those shown in Figs. 4*b* and 5*b*, our investigation does rule out a number of simple explanations and trivial artifacts which could otherwise be invoked to interpret subunit structures seen in these micrographs:

(*a*) Resolution per se is not improved by rotary shadowing; both unidirectional and rotary-replicated platinum-carbon anode replicas of polyheads resolve 25 Å periodicities. However, direct inspection and optical analysis show that only rotary replication is comparable to negative staining in contrasting specimen structure in a radially symmetrical fashion.

(*b*) Platinum recrystallization in the electron microscope cannot explain the rotary shadow image. Within the resolution limits we attained, recrystallization affected neither the quality of the replica nor its information content. This very surprising result suggests that the reorientation of platinum atoms, which must accompany the recrystallization detected by electron diffraction,[2] occurs within the boundaries of preexisting grains formed before the replica is placed in the electron beam. Although we cannot, without using minimal irradiation techniques, rule out the possibility that the electron dosage required for one photograph was sufficient to form the characteristic replica grains, discussions that directly equate heavy metal crystallization with resolution or replica grain size are clearly misleading (see also 14).

(*c*) Grains are unlikely to develop in patterns totally unrelated to underlying structure. Although we must reckon with decoration artifacts and random grain development, such phenomena do not account for our observation that in erythrocyte ghosts the intramembrane particles frequently appear to have a tetrameric arrangement of subunits,[3] whereas similar or even smaller-sized capsomeres in polyheads show their hexamer subunit configuration.

The striking similarity between our filtered negative images of shadowed polyheads (Fig. 8*a*, and *b*) and the positive image of a negatively stained polyhead (Fig. 8*c*) indicates that heavy metal can contrast structural features in a manner that is the opposite of negative staining. In other words, whereas negative stain tends to accumulate in depressions, platinum appears to condense upon or decorate small protruding structures (1, 14). This observation suggests several possible explanations for the improved detail seen in rotary replicated freeze-fractured membranes:

(*a*) It is generally accepted that surface imperfections and discontinuities drive the decoration processes of condensation and grain development (4, 10). When intramembrane particles are symmetrically replicated from all sides by

[2] Recrystallization of thin films in general takes place after interaction with the electron beam and is attributed largely to electronic processes rather than temperature (5).

[3] Whether plastic distortion (6) contributes to the particle heterogeneity observed in fractured membranes (Fig. 4*b*) remains to be clarified.

FIGURE 6 (*a*) A unidirectionally shadowed freeze-etched polyhead and (*b*) its optical diffraction pattern indexed according to the expected hexagonal lattice. Note that some of the first, second, third, and fourth order spots of the lattice have been resolved, corresponding to 110, 50, 35, and 25 Å, respectively. This polyhead was optimally oriented so that its unidirectional shadow provided the best detail of polyhead surface structure we have obtained with unidirectional shadowing. Bar, 0.1 μm (× 210,000).

FIGURE 7 (*a*) A rotary replicated freeze-etched polyhead and (*b*) its optical diffraction pattern. Observe that most of the first, second, third, and fourth order spots have been resolved corresponding to 110, 50, 35, and 25 Å, respectively. Polyheads showing this level of surface detail were routinely observed with rotary replication. Bar, 0.1 μm (× 210,000).

FIGURE 8 Filtered images of (*a*) unidirectionally shadowed polyhead shown in Fig. 6*a*; (*b*) rotary replicated polyhead shown in Fig. 7*a*; and (*c*) near side, negatively stained polyhead (reproduced from Fig. II*b*, DeRosier and Klug, 1972). To facilitate comparison with this negatively stained image, the images in (*a*) and (*b*) were printed to show Pt deposits in white. Bar, 500 Å (× 400,000).

the evaporated metal, decoration of underlying structure may be more faithful.

(*b*) Rotary-replicated particles do not cast true shadows on their neighbors, and pileup of replica material on one side of a surface protrusion is avoided. Thus, a rotary-replicated particle appears to be smaller and more discretely separated from its neighbors than a unidirectionally shadowed particle (compare in Fig. 5 parts *a* with *b*). Similarly, each of the subunits in a single particle may be more easily discriminated from its neighbors.

(*c*) Even when very thin replicas are cast, the contrast with which small surface features stand out is enhanced by a low angle of replication because large areas of the specimen which are lower than their surroundings receive hardly any metal deposit. With unidirectional shadowing, some of the advantages of low angle replicas are lost because the extended shadow cast by even a small protrusion may obscure a contiguous protrusion. Since this is not true with rotary replication, the full benefits of thin, low angle replication may be realized.

We cannot determine which, if any, of the above possibilities best explains our results. Other effects common to many replication techniques, such as differential grain development on lipids and proteins, may also contribute to the images. Although experience with other specimens as well as further tests with model systems are needed to clarify the mechanism of shadowing and replication, our experience to date, albeit limited, indicates that rotary replication can provide useful and interpretable images of freeze-etched specimens.

Although the equipment required to perform rotary replication is not elaborate,[1a] the technique is not a substitute for routine unidirectional shadowing which is adequate for many purposes. Rather, rotary replication should be a useful adjunct to the standard replica-forming technique when radially symmetrical contrast and discrimination between small, contiguous elements is important.

We thank Dr. David DeRosier for use of his optical diffractometer equipment and for his guidance, Dr. U. D. Laemmli and Dr. J. R. Paulson for the generous provision of virus-infected bacteria, and Dr. Kenneth Miller for the provision of the chloroplast material.

This research was supported in part by grants from the National Institutes of Health, the National Science Foundation, the Energy Research and Development Administration, and Balzers, AG, Balzers, Liechtenstein.

Received for publication 26 May 1976, and in revised form 7 September 1976.

REFERENCES

1. ABERMANN, R., M. M. SALPETER, and L. BACHMANN. 1972. High resolution shadowing. *In* Principles and Techniques of Electron Microscopy. M. A. Hayat, editor. Van Nostrand Reinhold Co., New York. **2:** 197–217.
2. BACHMANN, L., W. H. ORR, T. N. RHODIN, and B. M. SIEGEL. 1960. Determination of surface structure using ultra-high vacuum replication. *J. Appl. Physiol.* **31:**1458–1462.
3. BACHMANN, L., R. ABERMANN, and H. P. ZINGSHEIM. 1969. Hochauflösende Gefrierätzung. *Histochemie.* **20:**133–142.
4. BERRY, R. W., P. M. HALL, and M. T. HARRIS. 1968. Thin Film Technology. D. Van Nostrand Co., Inc., New York. 706 pp.
5. CALBICK, C. T. 1964. Interaction of thin films with electron beams. *In* Physics of Thin Films. G. Hass and R. E. Thun, editors. Academic Press, Inc., New York. 63–145.
6. CLARK, A. W., and D. BRANTON. 1968. Fracture faces in frozen outer segments from the guinea pig retina. *Zeit. Zellforsch. Mikrosk Anat.* **91:**586–603.
7. DEROSIER, D. J., and A. KLUG. 1972. Structure of the tubular variants of the head of bacteriophage T4 (polyheads). I. Arrangement of subunits in some classes of polyheads. *J. Mol. Biol.* **65:**469–488.
8. DODGE, J. T., C. MITCHELL, and D. J. HANAHAN. 1963. The preparation and chemical characteristics of hemoglobin-free ghosts of human erythrocytes. *Arch. Biochem. Biophys.* **100:**119–130.
9. FISHER, K., and D. BRANTON. 1974. Applicaton of the freeze-fracture technique to natural membranes. *Methods Enzymol.* **32**(Pt. B):35–44.
10. HEAVENS, O. S. 1970. Thin Film Physics. Methuen and Co. Ltd., London. 152 pp.
11. LAEMMLI, U. K., and S. F. QUITTNER. 1974. Maturation of the head of bacteriophage T4. IV. The protein of the core of the tubular polyheads and in vitro cleavage of the head proteins. *Virology.* **62:**483–499.
12. MOOR, H. 1971. Recent progress in the freeze-etching technique. *Philos. Trans. R. Soc. Lond. B. Biol. Sci.* **261:**121–131.
13. VINES, R. F. 1941. The platinum metals and their alloys. E. M. Wise, editor. The International Nickel Co., Inc., New York. 141 pp.
14. ZINGSHEIM, H. P. 1972. Membrane structure and electron microscopy. The significance of physical problems and techniques. (Freeze-etching.) *Biochim. Biophys. Acta.* **265:**339–366.